

Activation of Sulfur- and Nitrogen-Containing Heterocycles by a Dinuclear Iridium Complex

David A. Vivic and William D. Jones*

Department of Chemistry, University of Rochester, Rochester, New York 14627-0216

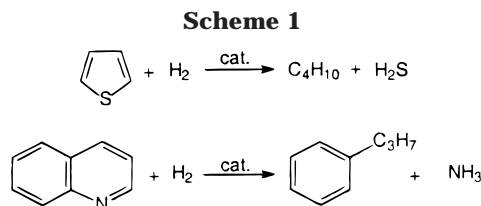
Received September 24, 1998

$[\text{Cp}^*\text{IrH}_3]_2$ was found to activate both nitrogen- and sulfur-containing heterocycles in the presence of a hydrogen acceptor, giving novel dinuclear organometallic products. In the case of 2-methylthiophene, C–S activation occurred along with a concomitant double hydride transfer and olefin migration to yield a stable adduct. C–H activation α to the heteroatom was observed for *N*-methylpyrrole, and a pyrrole complex containing a rare Ir–Ir triple bond was also isolated. All heterocycle adducts have been structurally characterized.

Introduction

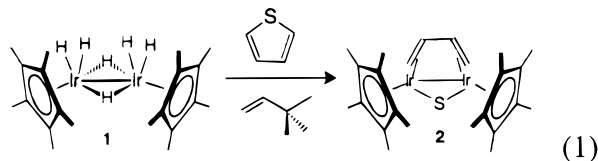
The removal of heteroatom impurities is an essential component of the refinement of crude oils.¹ In the hydrodesulfurization (HDS) process, crude oils are treated with high pressures of hydrogen (150–2250 psi) over a hot heterogeneous catalyst (320–440 °C) to remove sulfur impurities prior to further processing. Nitrogen-containing impurities are also removed under these conditions, in a process known as hydrodenitrogenation (HDN).² The heteroatom compounds, if not removed, can release SO_x and NO_x upon fuel combustion and contribute to acid rain production. Hence, their removal is of great environmental importance. Typical examples of HDS and HDN reactions are given in Scheme 1, which show the sulfur and nitrogen atoms being removed as H_2S and NH_3 .

Because of new regulations designed to limit the sulfur content in diesel fuels, much interest has been focused on the problems of “deep” hydrodesulfurization (HDS), or production of gas oils containing less than 0.05 wt % sulfur.³ These strict regulations are pushing industry to achieve a better understanding of the mechanism of HDS in attempts to design more efficient desulfurization catalysts. Since homogeneous modeling of the HDS reaction can allow researchers to analyze



specific steps in the HDS cycle, much effort has been put forth to study the HDS process in solution.⁴ Modeling work has primarily focused on understanding the reactivity of transition-metal complexes with thiophenic compounds, since these are the most difficult substrates to desulfurize in the hydroprocessing of crude oil.

Our laboratory has been studying polynuclear organometallic complexes as models for the HDS reaction, since there is compelling evidence that more than one metal center may be involved in the cleavage of both C–S bonds of thiophenes.⁵ Of relevance to the present work, the dinuclear iridium complex $[\text{Cp}^*\text{IrH}_3]_2$ (**1**) was previously found to react with thiophene in the presence of a hydrogen acceptor to afford the desulfurization product $[\text{Cp}^*\text{Ir}]_2(\mu\text{-S})(\mu\text{-}(1,2\text{-}\eta):(3,4\text{-}\eta)\text{-C}_4\text{H}_6)$ (**2**) (eq 1).^{5a} Further reaction of **2** with hydrogen produced butane.



(1) (a) Topsøe, H.; Clausen, B. S.; Massoth, F. E. *Hydrotreating Catalysis*; Springer-Verlag: Berlin, 1996. (b) Chianelli, R. R.; Daage, M.; Ledoux, M. J. *Adv. Catal.* **1994**, *40*, 177.

(2) (a) Katzer, J. R.; Sivasubramanian, R. *Catal. Rev.-Sci. Eng.* **1979**, *20*, 155. (b) Prins, R.; de Beer, V. H. J.; Somorjai, G. A. *Catal. Rev.-Sci. Eng.* **1989**, *31*, 1.

(3) (a) Unzelman, G. H.; *Oil Gas J.* **1987**, *19*(June), 55. (b) Takatsuka, T.; Wada, Y.; Suzuki, H.; Komatsu, S.; Morimura, Y. *Sekiyu Gakkaishi* **1992**, *35*, 179. (c) Shih, S. S.; Mizahi, S.; Green, L. A.; Sarli, M. S. *Ind. Eng. Chem. Res.* **1992**, *31*, 1232. (d) Topsøe, H.; Gates, B. C.; *Polyhedron* **1997**, *16*, 3212.

(4) (a) See, for example: Angelici, R. J. *Polyhedron* **1997**, *16*, 3073. (b) Bianchini, C.; Meli, A. *Acc. Chem. Res.* **1998**, *31*, 109. (c) Vivic, D. A.; Jones, W. D. *Organometallics* **1998**, *17*, 3411. (d) Iretskii, A.; Adams, H.; Garcia, J. J.; Picazo, G.; Maitlis, P. M. *Chem. Commun.* **1998**, 61. (e) Stafford, P. R.; Rauchfuss, T. B.; Verma, A. K.; Wilson, S. R. *J. Organomet. Chem.* **1996**, *526*, 203. (f) Harris, S. *Polyhedron* **1997**, *16*, 3219. (g) Zhang, X.; Dullaghan, C. A.; Carpenter, G. B.; Sweigart, D. W.; Meng, Q. *Chem. Commun.* **1998**, 93. (h) Curtis, M. D.; Druker, S. H. *J. Am. Chem. Soc.* **1997**, *119*, 1027. (i) Sargent, A. L.; Titus, E. P. *Organometallics* **1998**, *17*, 65. (j) Matsubara, K.; Okamura, R.; Tanaka, M.; Suzuki, H. *J. Am. Chem. Soc.* **1998**, *120*, 1108. (k) Reynolds, J. G. *Chem. Ind.* **1991**, 570. (l) Lopez, L.; Godziela, G.; Rakowski DuBois, M. *Organometallics* **1991**, *10*, 2660.

(5) (a) Jones, W. D.; Chin, R. M. *J. Am. Chem. Soc.* **1994**, *116*, 198. (b) Vivic, D. A.; Jones, W. D. *Organometallics* **1997**, *16*, 1912. (c) Jones, W. D.; Vivic, D.; Chin, R. M.; Roache, J.; Myers, A. *Polyhedron* **1997**, *16*, 3115. (d) Vivic, D. A.; Jones, W. D. *J. Am. Chem. Soc.* **1997**, *119*, 10857. (e) Riaz, U.; Curnow, O.; Curtis, M. D. *J. Am. Chem. Soc.* **1991**, *113*, 1416.

(6) (a) Bianchini, C.; Casares, J. A.; Masi, D.; Meli, A.; Pohl, W.; Vizza, F. *J. Organomet. Chem.* **1997**, *541*, 143. (b) Sánchez-Delgado, R. A. *J. Mol. Catal.* **1994**, *86*, 287. (c) Myers, A. W.; Jones, W. D. *Organometallics* **1996**, *15*, 2905. (d) Oglivly, A. E.; Draganjac, T. B.; Rauchfuss, T. B.; Wilson, S. R. *Organometallics* **1988**, *7*, 1171. (e) Isoda, T.; Nagao, S.; Korai, Y.; Mochida, I. *Sekiyu Gakkaishi* **1998**, *41*, 22. (f) Bianchini, C.; Jiménez, M. V.; Meli, A.; Vizza, F. *Organometallics* **1995**, *14*, 4858. (g) García, J. J.; Arevalo, A.; Capella, S.; Chehata, A.; Hernandez, M.; Montiel, V.; Picazo, G.; Del Río, F.; Toscano, R. A.; Adams, H.; Maitlis, P. M. *Polyhedron* **1997**, *16*, 3185.

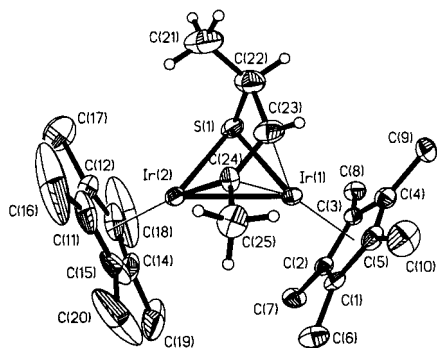
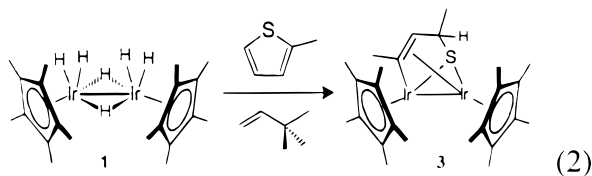


Figure 1. ORTEP drawing of $[\text{Cp}^*\text{Ir}]_2(\text{SC}_5\text{H}_8)$ (**3**). Ellipsoids are shown at the 30% probability level. Hydrogen atoms on the Cp^* ligands are omitted for clarity. Selected bond lengths (Å): C(21)–C(22), 1.46(2); C(22)–C(23), 1.51(2); C23–C24, 1.38(2); C(24)–C(25), 1.50(1). Selected bond angles (deg): C(24)–C(23)–C(22), 118.4(11); C(23)–C(24)–C(25), 120.2(9); C(21)–C(22)–C(23), 117.9(11); Ir(2)–C(24)–Ir(1), 79.8(3).

It was of interest to see if **1** could activate more sterically hindered thiophenes, since such compounds are found to be less reactive toward desulfurization.⁶ We were also curious to see if **1** showed reactivity toward nitrogen-containing heterocycles, since the salient features of the HDN process are still not very well-understood.^{4a,7}

Results and Discussion

Reaction of **1** with 2-methylthiophene in the presence of *tert*-butylethylene in THF (27 h, 55 °C) afforded a new organometallic product (**3**) as determined by ¹H NMR spectroscopy. **3** could be isolated in 41% yield after column chromatography as a bright red crystalline solid. X-ray-quality crystals were grown by dissolving **3** in diethyl ether and slowly cooling the solution to –30 °C. An X-ray analysis of the product revealed, in contrast to the reaction of **1** with unsubstituted thiophene, that both carbon–sulfur bonds were not cleaved under the above reaction conditions. Instead, a double hydride transfer reaction occurred with olefin migration, rendering a dinuclear species with both a bridging sulfur and carbon atom (eq 2). To our knowledge, such a rear-

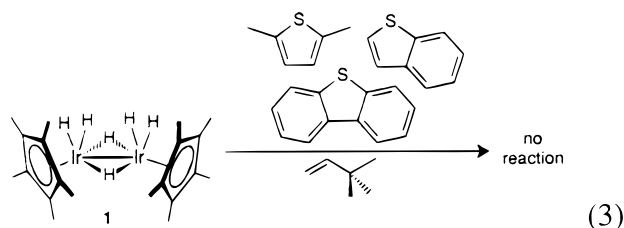


angement is unprecedented in HDS modeling studies. An ORTEP drawing of **3** is shown in Figure 1, with crystallographic data in Table 1. Other minor products were seen in the NMR spectrum of the crude reaction mixture but were not identified.

The X-ray data show that, similar to the case for compound **2**,^{5a} there is a substantial metal–metal interaction characterized by the Ir–Ir bond distance of 2.7263(5) Å (2.818 Å in **2**). The distances of the bridging sulfur atom to the iridium centers (2.327(2), 2.305(2)

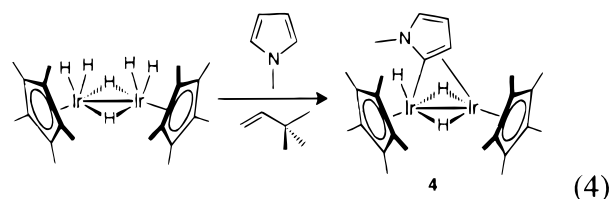
Å) also compare favorably to those seen in **2** (2.320(9), 2.318(8) Å) and to those in the known structures $[\text{Cp}^*\text{IrCl}]_2(\mu\text{-H})(\mu\text{-SC}_4\text{H}_9)$ (2.335(2), 2.337(2) Å) and $[\text{Cp}^*\text{IrCl}]_2(\mu\text{-H})(\mu\text{-S}(\text{C}_6\text{H}_4)\text{C}_2\text{H}_5)$ (2.345(1), 2.352(1) Å).^{5b}

When a THF solution of **3** was heated to 150 °C under 600 psig of H₂, cleavage of both C–S bonds was seen, yielding *n*-pentane as the desulfurized organic product (57%). It is interesting to note that both thiophene and 2-methylthiophene were desulfurized by the same organometallic compound apparently via different mechanisms involving **2** and **3** as intermediates, respectively, although it is difficult to rule out that these types of species interconvert under desulfurization conditions. Such reactions provide useful information for HDS catalysis, as they demonstrate how a given catalyst responds to changes in substrate structure. With the more refractory thiophenes such as 2,5-dimethylthiophene, benzothiophene, and dibenzothiophene, no reaction with **1** occurred (eq 3). This is unfortunate,



because related compounds, namely the alkylated dibenzothiophenes, are the most difficult compounds to remove in the hydroprocessing of crude oil and information that could lead to their removal is of tremendous value.^{4c}

The reactivity of a nitrogen-containing heterocycle with **1** was also investigated. Reaction of **1** with *N*-methylpyrrole in the presence of *tert*-butylethylene in cyclohexane (27 h, 55 °C) yielded a new organometallic complex (**4**) in 22% isolated yield after chromatography. As before, other minor products were seen in the NMR spectrum of the crude reaction mixture but were not identified. As determined by X-ray crystallography, the iridium complex did not cleave the carbon–nitrogen bonds of the pyrrole but instead activated the C–H bond at the α position (eq 4). An ORTEP drawing of **4** can be



seen in Figure 2, with crystallographic data in Table 1. The dinuclear structure has one iridium atom σ -bound to the α -carbon, while the other iridium center binds to the olefinic portion of the pyrrole in an η^2 fashion. While the hydride ligands were not reliably located by X-ray analysis,⁸ they can be observed in the ¹H NMR spectrum (cyclohexane-*d*₁₂) as three broad singlets at δ –16.95,

(8) Of the four largest residual electron density peaks, three were observed in positions corresponding to the structure shown in **4**. In light of the presence of two heavy atoms, however, these peaks were not taken as proof of the hydride locations.

(7) For recent reviews on the HDN reaction, see: (a) Weller, K. J.; Fox, P. A.; Gray, S. D.; Wigley, D. E. *Polyhedron* **1997**, *16*, 3139. (b) Prins, R.; Jian, M.; Flechsengar, M. *Polyhedron* **1997**, *16*, 3235.

Table 1. Crystallographic Data for 3–5

| | 3 | 4 | 5 |
|--|---|---|---|
| Crystal Parameters | | | |
| chem formula | C ₂₅ H ₃₈ Ir ₂ S | C ₂₅ H ₃₉ Ir ₂ N | C ₂₅ H ₃₇ Ir ₂ N |
| fw | 755.01 | 738.03 | 735.96 |
| cryst syst | monoclinic | monoclinic | monoclinic |
| space group (No.) | <i>P</i> 2 ₁ / <i>c</i> | <i>Cc</i> | <i>P</i> 2 ₁ |
| <i>Z</i> | 4 | 4 | 2 |
| <i>a</i> , Å | 10.8636(3) | 16.4804(3) | 8.4912(5) |
| <i>b</i> , Å | 14.1074(4) | 15.3201(3) | 14.1404(8) |
| <i>c</i> , Å | 16.6979(4) | 9.8855(10) | 10.3010(6) |
| β , deg | 100.14 | 98.69 | 104.93 |
| <i>V</i> , Å ³ | 2519.09(12) | 2467.23(7) | 1195.08(12) |
| ρ_{calcd} , g cm ⁻³ | 1.991 | 1.989 | 2.045 |
| cryst dims, mm ³ | 0.40 × 0.40 × 0.20 | 0.26 × 0.26 × 0.08 | 0.35 × 0.30 × 0.15 |
| temp, °C | -50 | -50 | -50 |
| Measurement of Intensity Data | | | |
| diffractometer | Siemens SMART | Siemens SMART | Siemens SMART |
| radiation (λ , Å) | Mo (0.710 73) | Mo (0.710 73) | Mo (0.710 73) |
| frame range/time, deg/s | 0.3/30 | 0.3/10 | 0.3/10 |
| 2 θ range, deg | 3.8–56.6 | 3.6–56.7 | 4.1–48.0 |
| data collected | -13 ≤ <i>h</i> ≤ 14 -15 ≤ <i>k</i> ≤ 18 -22 ≤ <i>l</i> ≤ 18 | -21 ≤ <i>h</i> ≤ 21 -20 ≤ <i>k</i> ≤ 15 -12 ≤ <i>l</i> ≤ 11 | -11 ≤ <i>h</i> ≤ 11 -14 ≤ <i>k</i> ≤ 18 -13 ≤ <i>l</i> ≤ 13 |
| no. of data collected | 15 369 | 7598 | 5557 |
| no. of unique data | 5930 | 4834 | 2989 |
| no. of obsd data ($F_o > 2\sigma(F_o)$) | 5073 | 4143 | 2446 |
| agreement between equiv data (R_{int}) | 0.0299 | 0.0353 | 0.0471 |
| no. of params varied | 361 | 254 | 269 |
| μ , mm ⁻¹ | 10.646 | 10.786 | 11.134 |
| abs cor | SADABS | SADABS | SADABS |
| range of transmissn factors | 0.928–0.481 | 0.928–0.418 | 0.928–0.380 |
| R1(F_o), wR2(F_o^2) ($F_o > 4\sigma(F_o)$) | 0.0448, 0.1119 | 0.0410, 0.0939 | 0.0398, 0.0898 |
| R1(F_o), wR2(F_o^2) (all data) | 0.0541, 0.1163 | 0.0501, 0.0985 | 0.0456, 0.0920 |
| goodness of fit | 1.081 | 0.974 | 1.087 |

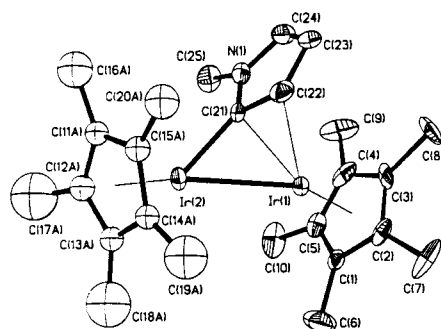
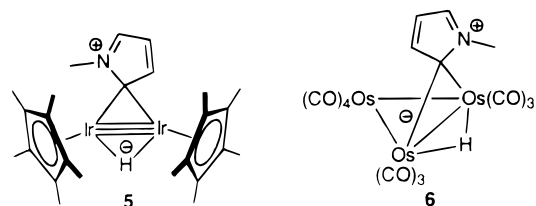


Figure 2. ORTEP drawing of [Cp*Ir]₂(C₅H₆N) (**4**). All hydrogen atoms have been omitted for clarity. Selected bond lengths (Å): Ir(1)–Ir(2), 2.7945(5); Ir(1)–C(21), 2.217(13); Ir(1)–C(22), 2.315(13); Ir(2)–C(21), 2.028(14); N(1)–C(21), 1.41(2); N(1)–C(24), 1.36(2); C(21)–C(22), 1.44(2); C(22)–C(23), 1.44(2); C(23)–C(24), 1.36(2). Selected bond angles (deg): C(21)–Ir(1)–Ir(2), 46.0(4); C(22)–Ir(1)–Ir(2), 73.3(3); C(22)–C(21)–Ir(2), 125.3(11); C(22)–C(21)–Ir(1), 76.8(8); Ir(2)–C(21)–Ir(1), 82.2(4).

–18.14, and –19.24. The solution-state structure of **4** is therefore proposed to contain two bridging hydrides and one terminal hydride. Two alternate structures are possible, one in which the terminal hydride is moved to the other iridium center or a second in which there

would be only one bridging hydride ligand with a terminal hydride on each metal center.

Flushing the chromatography column with methanol afforded a second organometallic product in trace amounts. The green complex **5** was identified by X-ray crystallography and was found to be a rare example of a complex containing an iridium–iridium triple bond.



An ORTEP drawing of **5** is shown in Figure 3, with crystallographic data in Table 1. The short Ir–Ir bond length of 2.462 Å compares favorably to previously reported iridium–iridium triple bonds of 2.518 Å for [Ir₂(μ-H)₃H₂(PPh₃)₄]PF₆⁹ and 2.465 Å for [(Cp*Ir)₂(μ-H)₃]ClO₄¹⁰ and is much shorter than reported Ir–Ir double-bond lengths of ca. 2.575 Å.¹¹ A similar zwitterionic binding mode of *N*-methylpyrrole to transition metals was observed by Deeming and co-workers (compound **6**), who examined pyrrole activation with osmium and ruthenium clusters.¹²

Conclusions

[Cp*IrH₃]₂ (**1**) was found to activate 2-methylthiophene and *N*-methylpyrrole under mild thermal

(9) Crabtree, R. H.; Felkin, H.; Morris, G. E.; King, T. J.; Richards, J. A. *J. Organomet. Chem.* **1976**, *113*, C7.

(10) Stevens, R. C.; Mclean, M. R.; Wen, T.; Carpenter, J. D.; Bau, R.; Koetzle, T. F. *Inorg. Chim. Acta* **1989**, *161*, 223.

(11) (a) Arif, A. A.; Jones, R. A.; Schwab, S. T.; Whittlesey, B. R. *J. Am. Chem. Soc.* **1986**, *108*, 1703. (b) Arif, A. A.; Heaton, D. E.; Jones, R. A.; Kidd, K. B.; Wright, T. C.; Whittlesey, B. R.; Atwood, J. L.; Hunter, W. E.; Zhang, H. *Inorg. Chem.* **1987**, *26*, 4065. (c) Bleeke, J. R.; Rohde, A. M.; Robinson, K. E. *Organometallics* **1994**, *13*, 401. (d) Bleeke, J. R.; Rohde, A. M.; Robinson, K. E. *Organometallics* **1995**, *14*, 1674.

(12) (a) Arce, A. J.; Machado, R.; De Sanctis, Y. D.; Capparelli, M. V.; Atencio, R.; Manzur, J.; Deeming, A. J. *Organometallics* **1997**, *16*, 1735. (b) Deeming, A. J.; Arce, A. J.; De Sanctis, Y. D.; Day, M. W.; Hardcastle, K. I. *Organometallics* **1989**, *8*, 1408.

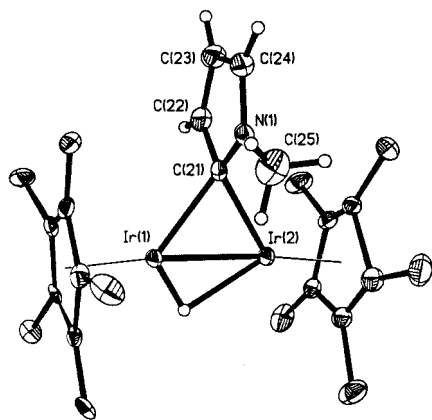


Figure 3. ORTEP drawing of **5**. Ellipsoids are shown at the 30% level. Hydrogen atoms on the Cp* ligands are omitted for clarity. Selected bond lengths (Å): Ir(1)–Ir(2), 2.4628(5); Ir(1)–C(21), 2.161(13); Ir(2)–C(21), 2.169(13); N(1)–C(24), 1.35(2); N(1)–C(21), 1.36(2); C(21)–C(22), 1.44(2); C(22)–C(23), 1.38(3); C(23)–C(24), 1.36(3). Selected bond angles (deg): Ir(1)–C(21)–Ir(2), 69.3(4); N(1)–C(21)–C(22), 103.4(13); N(1)–C(24)–C(23), 109.1(14); C(22)–C(23)–C(24), 106(2); C(23)–C(22)–C(21), 109(2).

conditions. In all cases, the products were stable upon column chromatography, which allowed for the isolation of analytically pure material suitable for X-ray analysis. The 2-methylthiophene adduct (**3**) could be desulfurized at high temperatures and under high pressures of hydrogen, which is consistent with the notion that participation of more than one metal center facilitates the desulfurization process. Carbon–nitrogen bond cleavage was not observed for the reaction of **1** with *N*-methylpyrrole. Similar reactivity toward heterocycles has been seen in the commercial hydrotreating process, where the highly effective HDS catalyst (CoMo/Al₂O₃) shows less activity for HDN.^{4a}

Experimental Section

General Procedures. All operations were performed under a nitrogen atmosphere unless otherwise stated. Cyclohexane, diethyl ether, and THF were distilled from dark purple solutions of benzophenone ketyl. Neutral alumina was heated to 200 °C under vacuum for 2 days and stored under nitrogen. 2-Methylthiophene (99+%) was purchased from Aldrich Chemical Co. and purified as previously reported.¹³ [Cp*IrH₃]₂ was prepared as previously reported.^{5a} *tert*-Butylethylene (95%) was purchased from Aldrich Chemical Co. and distilled over molecular sieves. A Siemens SMART Area Detector was used for X-ray crystal structure determination. Elemental analyses were obtained from Desert Analytics. All ¹H NMR spectra were recorded on a Bruker AMX400 NMR spectrometer, and chemical shifts are reported relative to the residual proton resonance in the deuterated solvent. High-pressure reactions were performed with a Parr 4702 bomb equipped with a Teflon liner.

Preparation of [Cp*Ir]₂C₅H₈S (3**).** [Cp*IrH₃]₂ (130 mg, 0.197 mmol), 2-methylthiophene (0.93 mL, 9.61 mmol), and 3,3-dimethyl-1-butene (0.37 mL, 2.87 mmol) were dissolved in 3 mL of THF and placed in an ampule fitted with a Teflon valve. The solution was heated at 55 °C for 27 h, and then all volatiles were removed under vacuum. The residue was then passed through a neutral alumina column using hexanes/ether (98:2) as an eluent. The solvents of the first red band were removed under vacuum, leaving a red solid (61 mg, 41%). ¹H NMR (400 MHz, C₆D₁₂, 25 °C): δ 2.86 (dq, *J* = 6.4, 2.9 Hz, 1

H), 2.04 (s, 3H), 2.06 (d, *J* = 3.1 Hz, 1 H), 2.03 (s, 15 H), 1.87 (s, 15 H), 0.32 (d, *J* = 6.2 Hz, 3 H). Anal. Calcd (found) for C₂₅H₃₈Ir₂S: C, 39.77 (39.84); H, 5.07 (5.15). Mass spectrum (direct inlet EI, 70 eV): 756 (M⁺).

Preparation of [Cp*Ir]₂H₃(C₅H₆N) (4**) and [Cp*Ir]₂H₃(C₅H₆N) (**5**).** [Cp*IrH₃]₂ (125 mg, 0.189 mmol) was dissolved in *N*-methylpyrrole (0.7 mL, 7.88 mmol), 3,3-dimethyl-1-butene (0.5 mL, 3.88 mmol), and 4 mL of cyclohexane and placed in an ampule fitted with a Teflon valve. The solution was heated to 55 °C for 27 h, and then all volatiles were removed under vacuum. The residue was passed through a neutral alumina column using pentane/ether (99:1) as eluent. The golden band was collected and the solvents removed under vacuum, leaving an orange solid (30 mg, 22%). ¹H NMR (400 MHz, C₆D₁₂): δ 7.14 (dd, *J* = 1.5, 3.0 Hz, 1H), 5.53 (t, *J* = 2.5 Hz, 1H), 5.36 (m, 1H), 3.13 (s, 3H), 1.98 (s, 15H), 1.64 (s, 15H), –16.95 (br s, 1H), –18.14 (br s, 1H), –19.24 (br s, 1H). Anal. Calcd. (found) for C₂₅H₃₉Ir₂N: C, 40.69 (40.04); H, 5.33 (5.05); N, 1.90 (1.90). Compound **5** was isolated by flushing the column with methanol and collecting the green fraction. Yield: 6 mg. ¹H NMR (400 MHz, C₆D₁₂): δ 6.77 (dd, *J* = 2.9, 1.4 Hz, 1H), 6.00 (m, 1H), 5.77 (t, *J* = 2.9 Hz, 1H), 3.06 (s, 3H), 1.79 (s, 30H), –18.43 (s, 1H).

Hydrogenation of **3.** [Cp*Ir]₂SC₅H₈ (46 mg, 0.06 mmol), cyclohexane (2 μL), and THF-*d*₈ (0.9 mL) were placed in a Parr bomb, and 600 psig of H₂ was added. The solution was heated for 19 h at 150 °C. The vessel was cooled to room temperature, depressurized, and analyzed for pentane relative to cyclohexane by ¹H NMR spectroscopy. NMR yield of pentane: 57%.

X-ray Structural Determination of [Cp*Ir]₂(C₅H₈S) (3**).** Slow cooling of a solution of **3** in diethyl ether produced orange plates. A single crystal of dimensions 0.40 × 0.40 × 0.20 mm³ was mounted on a glass fiber with epoxy. Data were collected at –50 °C on a Siemens SMART CCD area detector system employing a 3 kW sealed-tube X-ray source operating at 1.5 kW. A total of 1.3 hemispheres of data were collected over 14 h, yielding 5930 observed data after integration using SAINT (see Table 1). Laue symmetry revealed a primitive monoclinic crystal system, and cell parameters were determined from 5073 unique reflections.¹⁴ The space group was assigned as *P*2₁/*c* on the basis of systematic absences and intensity statistics using XPREP, and the structure was solved and refined using direct methods included in the SHELXTL 5.04 package. For a *Z* value of 4 there is one independent molecule within the asymmetric unit. In the final model, non-hydrogen atoms were refined anisotropically (on *F*²), with hydrogens included in idealized locations. The structure was refined to R1 = 0.0448 and wR2 = 0.1119.¹⁵ Fractional coordinates and thermal parameters are given in the Supporting Information.

X-ray Structural Determination of [Cp*Ir]₂H₃(C₅H₆N) (4**).** Slow evaporation of a hexanes solution of **4** produced orange plates. A single crystal of dimensions 0.26 × 0.26 × 0.08 mm³ was mounted on a glass fiber with epoxy. Data were collected at –50 °C on a Siemens SMART CCD area detector system employing a 3 kW sealed-tube X-ray source operating at 1.5 kW. A total of 1.3 hemispheres of data were collected over 7 h, yielding 4834 observed data after integration using SAINT (see Table 1). Laue symmetry revealed a *C*-centered monoclinic crystal system, and cell parameters were determined from 4143 unique reflections. The space group was assigned as *Cc* on the basis of systematic absences and intensity statistics using XPREP, and the structure was solved and refined using direct methods included in the SHELXTL 5.04 package. For a *Z* value of 4 there is one independent

(14) It has been noted that the integration program SAINT produces cell constant errors that are unreasonably small, since systematic error is not included. More reasonable errors might be estimated at 10× the listed values.

(15) Using the SHELXTL 5.04 package, R1 = (Σ|F_o| – |F_c|)/Σ|F_o| and wR2 = [Σ[w(F_o² – F_c²)²]/Σ[w(F_o²)²]^{1/2}, where w = 1/[σ²(F_o²) + (aP)² + bP] and P = [f(maximum of 0 or F_o²) + (1 – f)F_c²].

(13) Spies, G. H.; Angelici, R. J. *Organometallics* **1987**, *6*, 1897.

molecule within the asymmetric unit. In the final model, non-hydrogen atoms were refined anisotropically (on F^2), with hydrogens included in idealized locations. One of the Cp* groups was disordered (50/50) over two positions and was refined as a pair of isotropic rigid groups. The structure was refined to $R1 = 0.0410$ and $wR2 = 0.0939$. Fractional coordinates and thermal parameters are given in the Supporting Information.

X-ray Structural Determination of [Cp*Ir]₂H(C₃H₆N) (5). Slow cooling of a hexanes solution of **5** in produced green prisms. A single crystal of dimensions $0.35 \times 0.30 \times 0.15$ mm³ was mounted on a glass fiber with epoxy. Data were collected at -50 °C on a Siemens SMART CCD area detector system employing a 3 kW sealed-tube X-ray source operating at 1.5 kW. A total of 1.3 hemispheres of data were collected over 7 h, yielding 2989 observed data after integration using SAINT (see Table 1). Laue symmetry revealed a primitive monoclinic crystal system, and cell parameters were determined from 2446 unique reflections. The space group was assigned as $P2_1$ on the basis of systematic absences and intensity statistics using XPREP, and the structure was solved and refined using

direct methods included in the SHELXTL 5.04 package. For a Z value of 2 there is one independent molecule within the asymmetric unit. In the final model, non-hydrogen atoms were refined anisotropically (on F^2), with hydrogens included in idealized locations. A bridging hydride ligand, located in a difference Fourier map, was included and refined isotropically. The structure was refined to $R1 = 0.0398$ and $wR2 = 0.0898$. Fractional coordinates and thermal parameters are given in the Supporting Information.

Acknowledgment is made to the National Science Foundation (Grant No. CHE-9421727) for their support of this work.

Supporting Information Available: Figures giving ¹H NMR spectra for **4** and **5** and tables of crystallographic data, atom coordinates, thermal parameters, and bond distances and angles for **3–5** (25 pages). Ordering information is given on any current masthead page.

OM9808007